

Adsorption and desorption of cadmium on synthetic schwertmannite

Lijun Fan*, Xiongjian Zhang

College of Geoscience and Surveying Engineering, China University of Mining & Technology, Beijing 100083, China, Tel. +86 15650763709; email: TSP130203060@student.cumt.edu.cn, TSP130201121Q@student.cumt.edu.cn

Received 5 June 2016; Accepted 31 October 2016

ABSTRACT

Cadmium is a toxic contaminant in environment, it is essential to remove Cd^{2+} from wastewater. This study has investigated the feasibility of using synthetic schwertmannite for Cd^{2+} removal from aqueous solution. Schwertmannite was synthesized by two methods, and characterized by XRD, SEM and FTIR. The slow synthetic schwertmannite was used for batch experiments, which were conducted under different Cd^{2+} concentrations, temperatures, pH and Cd^{2+} desorption ability at different pH was also investigated. Results showed that the Langmuir isotherm described the adsorption of Cd^{2+} well. Thermodynamic study manifested the adsorption was spontaneous and endothermic. The synthetic schwertmannite had high adsorption capacity for Cd^{2+} removal of 110 mg/g with an adsorbent dosage of 1 g/L and an initial pH 8.0 at 25°C. At pH > 6.0 cadmium adsorption was dramatically increased, nearly 100% cadmium was adsorbed at pH = 8.0. In natural pH range for schwertmannite, Cd^{2+} adsorbed in schwertmannite had a good regeneration ability, Cd^{2+} desorption proportion of total sorbed quantity was 50–80%, and the desorption rate increased with the decrease of pH. Therefore, Schwertmannite can be employed as an efficient adsorbent for the removal of cadmium from contaminated water.

Keywords: Cd^{2+} ; Schwertmannite; Adsorption; Desorption

1. Introduction

Heavy metal contamination due to developments in technology is one of the world-wide environment issue. It has high toxicity, bioaccumulation and biomagnifications effect, which imposed great concern to our environment [1]. Cadmium is a toxic contaminant in environment, it has been classified as a human carcinogen and teratogen, impacting the lungs, kidneys, liver and reproductive organs [2]. The harmful effects of cadmium include a number of acute and chronic disorders, such as renal damage, emphysema, hypertension and testicular atrophy [3]. Cadmium is principally dispersed in nature and environment through various agricultural, mining, industrial activities and the exhausts of automobiles [4–6]. With the increase of cadmium in environment, the content of cadmium in water has also increased. Therefore, it is essential to mitigate Cd^{2+} from water and wastewater prior

to transport in order to prevent it cycle into the natural environment. Cadmium removal from water can be achieved by chemical precipitation [7], ion exchange [8], electroflotation [9], reverse osmosis [10] and adsorption [11,12]. Among these methods, adsorption has been developed as an efficient method for the removal of heavy metals from contaminated water. A variety of conventional adsorbents, including clays, red mud, kaolin, metal oxides, activated carbon were used for cadmium removal [13,14]. Besides, many non-conventional adsorbents like *Setaria verticillata* Carbon, poly sulphate sponge, microorganisms, fly ash were used to reduce the many contaminants in the wastewater [15,16]. However, few studies had focused on Cd^{2+} removal using non-conventional adsorbents – schwertmannite. It was reported that the synthetic schwertmannite had a high adsorption capacity and good adsorption kinetics for removal of As [17,18], Cu [19,20], F [21,22], Cr [23,24]. Schwertmannite (ideally $\text{Fe}_8\text{O}_8(\text{OH})_6\text{SO}_4$) is a poorly crystalline iron oxyhydroxysul-

*Corresponding author.

fate that is stable under highly acidic conditions (2.5–4.5) and at high SO_4^{2-} concentrations [25–27]. It is a good adsorbent because of its extremely high surface area, adsorption capacity and reactivity. In this study, the removal feasibility of cadmium by synthetic schwertmannite had been investigated by batch experiments.

The main objectives were as follows: (i) to give insight into Cd^{2+} adsorption from thermodynamic views, (ii) to assess the impact of pH, temperature on Cd^{2+} removal, and (iii) to describe the adsorption-desorption ability of Cd^{2+} . In addition, the recycle of cadmium and schwertmannite due to the desorption ability of Cd^{2+} was discussed.

2. Materials and methods

2.1. Chemicals

All reagents were of analytical grade. Stock Cd^{2+} solution was 0.020 mol/L. Working cadmium solutions of required concentrations were prepared by appropriate dilution of the stock solution.

2.2. Synthesis of schwertmannite

Schwertmannite was synthesized by two different procedures: method 1 (slow synthesis) was described by Bigham et al. [28] and method 2 (rapid synthesis) was described by Regenspurg and Peiffer [29]. In method 1, 2000 mL pre-heated (60°C) deionized water was mixed with 10.8 g $\text{FeCl}_3 \cdot 6\text{H}_2\text{O}$ and 3 g Na_2SO_4 in a round-bottomed flask. The solution was kept further for 12 min at 60°C, and the fresh precipitates were cooled to room temperature. The precipitates were then centrifuged in 50 mL tube for 30 min at the speed of 2000 r/min. Afterwards, the mixture was dialyzed (Serva dialysis bags, ϕ 2.4 nm) in ~ 4.0 L of deionized water which was renewed four times daily. The conductivity of the dialysis water was found to be < 5 μS for the last 5 days indicating that ion exchange was ceased. Then freeze-dried before use. In method 2, 18.3 g $\text{FeSO}_4 \cdot 7\text{H}_2\text{O}$ was dissolved in 1 L deionized water and reacted with 5.3 mL 30% H_2O_2 . The solution became dark, and a red-orange material precipitated immediately with the final pH of 2.4 after 24 h. The solid was then centrifuged, washed and freeze-dried before use.

2.3. The adsorption preparation

Adsorption isotherm studies were carried out by reacting 0.5, 1.0, 2.5, 5.0, 25.0, 50.0 mL Cd^{2+} (0.020 mol/L) solution in 250 mL polyethylene bottles with 0.1 g adsorbent and 1 mL NaNO_3 (1 mol/L). NaNO_3 solution was used to provide a stable background of ionic strength (0.01 mol/L). The solution pH (i.e., 4.0, 5.0, 6.0, 7.0, 8.0) was adjusted by using HNO_3 (0.1 mol/L) or NaOH (0.1 mol/L) solutions at 25°C. The batch bottles were kept in a shaking water bath with a thermostatic controller at specified temperature for a predetermined contact time. The shaker speed was 180 rpm. After a predetermined contact time, the supernatant was decanted, centrifuged and filtered with 0.45 μm cellulose acetate membranes, and analyzed for residual Cd^{2+} concentrations.

To determine the effect of temperature on Cd^{2+} adsorption, the solution pH was 7.0. Batch tests were performed at 25 and 50°C.

2.4. The adsorption-desorption preparation

Schwertmannite (0.5 g) was added to 50.0 mL of 0.020 mol/L $\text{Cd}(\text{NO}_3)_2$ at pH 7.0, 25°C, and the ionic strength was 0.01 mol/L. The suspension pH was adjusted to 7.0 using concentrated NaOH or HNO_3 . Deionized water was added to the polyethylene bottles to make up to the 90 mL final volume. This suspension was shaken at 25°C, 180 r/min for 24 h and filtered through a 0.45 μm membrane. The filtrate Cd^{2+} adsorbed schwertmannite were dried, dispensed into 250 mL polyethylene bottles. The NaNO_3 (1 mol/L) solution and deionized water were added to make up to the 90 mL final volume.

Desorption experiments were performed at various pH (i.e., 2.5, 3.0, 3.5, 4.0, and 4.5). The solution pH was adjusted by the addition of NaOH or HNO_3 . Deionized water were added to make up to the 100 mL final volume, and shaken at 25°C, 180 r/min for 24 h. Then filtered through a 0.45 μm membrane.

2.5. Analytical methods

Standard pH meter (PHSJ-4A, Shanghai) was used for pH determination. Concentration of cadmium in solution was measured by flame atomic absorption spectroscopy (AAS). The crystalline structure of schwertmannite was characterized by X-ray diffraction (XRD, D/Max-2500, Rigaku) using an X-ray diffractometer fitted with a Cu X-ray source. Samples were scanned from $2\theta = 2.6$ – 80° , with a $2\theta = 0.01^\circ$ step size. Morphological analysis of the adsorbents was performed by Scanning electron microscopic (SEM, TESCAN VEGA II LMU, Europe) at 20 kV. The functional groups present in the adsorbent were analysed by Fourier transform infrared (FTIR, Vector 22, Bruker). The KBr pelleted samples were scanned over the wavenumber range 400–4000 cm^{-1} with resolution of 0.5 cm^{-1} .

3. Results and discussion

3.1. Characterization of synthesized schwertmannite

The XRD patterns of synthetic schwertmannite produced by both synthetic methods were shown in Fig. 1 XRD results showed that the two both synthesis schwertmannite did not have significant differences in crystalline structure.

FTIR spectrum showed that the vibrational bands in two synthetic schwertmannite were similar based on the number of obvious peaks and their positions. Infrared spectra of schwertmannite included absorption bands due to $\nu_1\text{-SO}_4^{2-}$ at 980 cm^{-1} , $\nu_4\text{-SO}_4^{1-}$ at 608 cm^{-1} , and $\nu_3\text{-SO}_4^{1-}$ at 1124, 1090, and 1050 cm^{-1} , respectively. These bands, along with those at 800–880 and 3410 cm^{-1} (OH stretching vibration), are typical of schwertmannite (Fig. 2).

SEM micrographs (Figs. 3, 4) showed both synthesis schwertmannite differ mostly in their surface characteristics: grains (or crystal aggregates) of slow synthesis were larger than rapid synthesis. And the slow synthesis crystal surface had compact-grain, while the rapid synthesis was

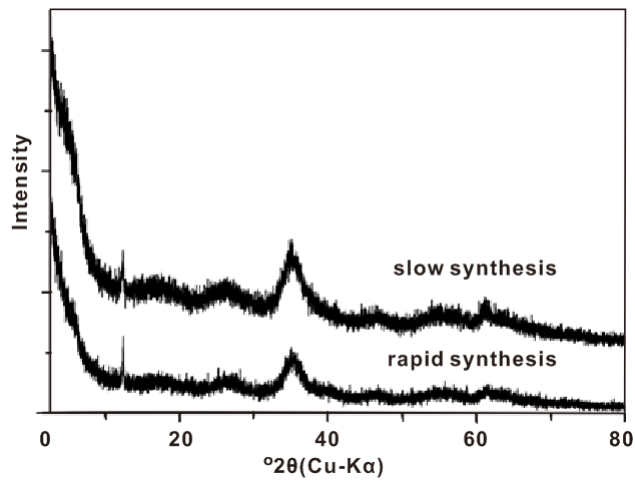


Fig. 1. XRD patterns of synthetic schwertmannite (produced by two synthesis methods).

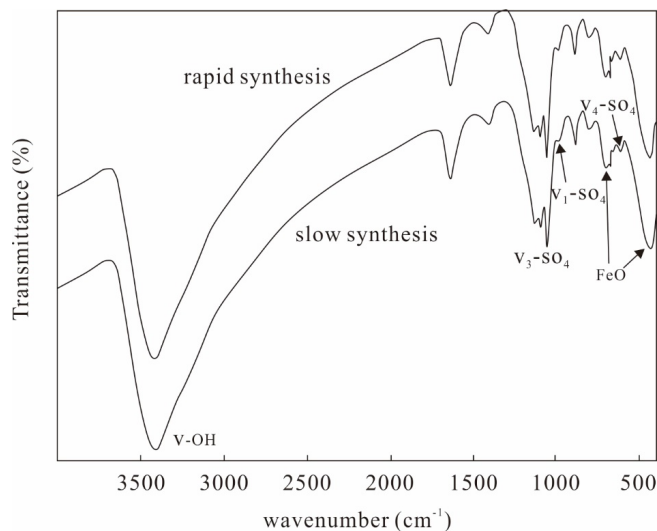


Fig. 2. FTIR-spectra of synthetic schwertmannite (produced by two synthesis methods).

porous. Both SEM micrographs were different from previous studies.

Regenspurg S. found that the specific surface area of slow synthesis was much larger compared to rapid synthesis. And the grains formed by rapid synthesis are large spheroids [29]. The slow synthesis method generated crystals, grew as long needles, which formed the characteristic “hedge-hog” habit of schwertmannite particles. The natural sample had a specific surface area of 72 m²/g and its morphology were resembled that of the specimen synthesized by the long-time experiment [29]. The wide difference in the two specimens surface area was related to their particle morphology, which was controlled by the synthesis pathway. As we know, high surface area had good probability of adsorption performance. The surface area was a key factor to schwertmannite adsorption of Cd²⁺, which determined the adsorption uptake. The batch experiments chose the slow synthesis schwertmannite. Why? The adsorption

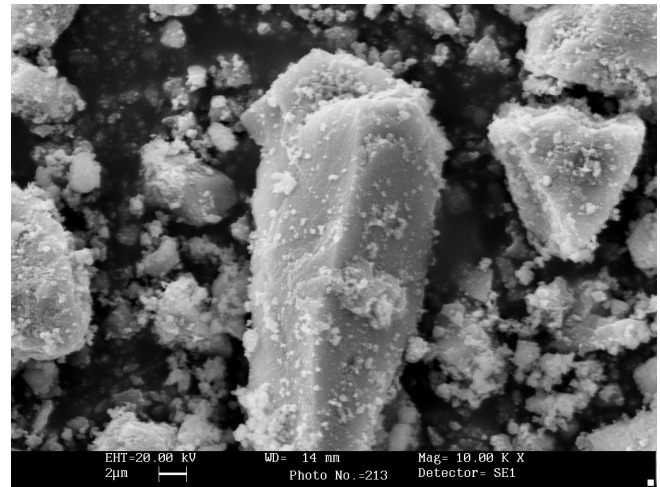


Fig. 3. SEM of schwertmannite in method 1 (slow synthesis).

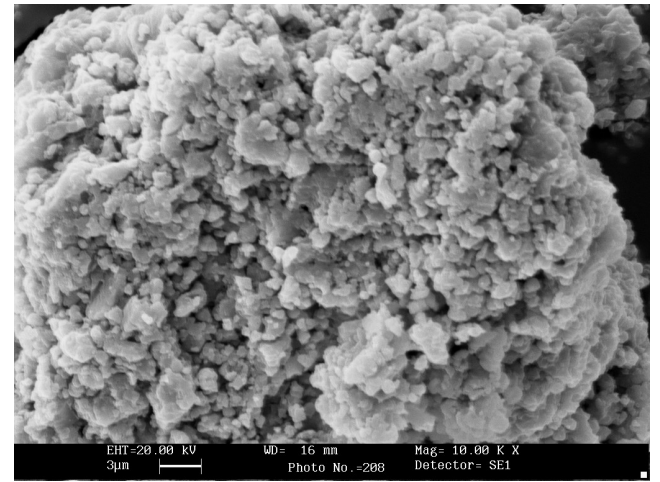


Fig. 4. SEM of schwertmannite in method 2 (rapid synthesis).

experiments were carried out using the slow synthetic schwertmannite due to its higher surface area. The fresh schwertmannite was crushed into powder (200 mesh), and kept in a desiccator. The powder was used as adsorbent for Cd²⁺ removal in the following studies.

3.2. The study of cadmium adsorption isotherms

The study of cadmium adsorption isotherm was tested with initial Cd²⁺ concentrations between 0.1 and 10 mmol/L, adsorbent dosage of 1 g/L, at pH 4.0, 5.0, 6.0, 7.0, and 8.0. The equilibrium adsorption capacity q (mg/g) is calculated by using the following equation:

$$q(\text{mg/g}) = \frac{c_0 - c}{m} \times V \times M \quad (1)$$

where c_0 is the initial concentration of Cd²⁺ (mmol/L); c is the equilibrium concentration of Cd²⁺ (mmol/L); m is adsorbent mass (g); V is the solution volume; M is atomic weight of cadmium (51.996 g/mol).

The equilibrium isotherm models would help to reveal the adsorption mechanism, the surface properties and affinity of the adsorbent. The experimental data of equilibrium isotherm for Cd^{2+} onto synthetic schwertmannite were modeled using the most frequently used Langmuir, Freundlich, and Temkin isotherms. The Langmuir equation, which assumed that homogeneous monolayer surface adsorption occurred, was expressed in the following equation:

$$q = q_{\max} \frac{kc}{1 + kc} \quad (2)$$

The Freundlich equation assumed a heterogeneous and patch-wise surface that was independent from one another and is expressed in the following equation:

$$q = kc^{1/n} \quad (3)$$

The Temkin isotherm considered the effects of indirect adsorbate/adsorbate interactions, which has been used in the form as follows:

$$q = a + b \ln c \quad (4)$$

where c is the equilibrium concentration of Cd^{2+} in aqueous phase (mg/L); q is the equilibrium adsorption capacity (mg/g); q_{\max} and k are the maximum adsorption capacity (mg/g) and adsorption equilibrium constant (L/mg) in Langmuir isotherms, respectively; k and $1/n$ are empirical constants of Freundlich isotherms, indicating the adsorption capacity and adsorption intensity, respectively; Temkin isotherm has two isotherm constants a and b .

The adsorption data were fitted to the three models. The plots of Langmuir, Freundlich and Temkin isotherms are shown in Figs. 5–7. The correlation coefficients and constants for Langmuir, Freundlich, and Temkin isotherms at various temperatures are summarized in Table 1.

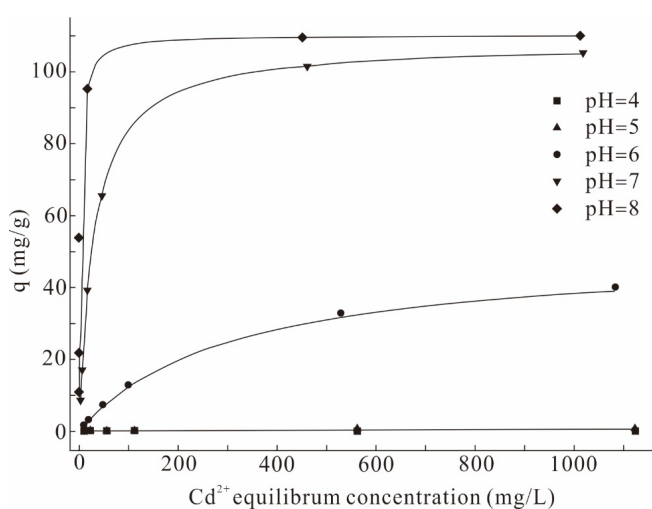


Fig. 5. Langmuir isotherm model fits to the cadmium sorption data (adsorbent dosage = 1 g/L, ionic strength = 0.01 mol/L, $T = 25^\circ\text{C}$, initial Cd^{2+} concentrations = 0.1–10 mmol/L, pH = 4.0–8.0).

It was observed that there were higher correlation coefficients for Langmuir isotherm than both Freundlich and Temkin isotherm, indicating that Cd^{2+} adsorption closer followed Langmuir isotherm and presented a monolayer adsorption trend [30]. The adsorption capacity indicated the same trend with the increase of pH, and the maximum removal capacity (Fig. 7) was 110 mg/g. This was much higher than the adsorption capacity of other adsorbents reported in the literature. A comparison of the schwertmannite with other adsorbents are shown in Table 2. It indicated that schwertmannite had a relatively good adsorption abilities than many other reported adsorbents (except phosphogypsum).

3.3. Effect of solution pH

The solution pH strongly affects the adsorption process, the adsorbent surface charge, the ionization degree

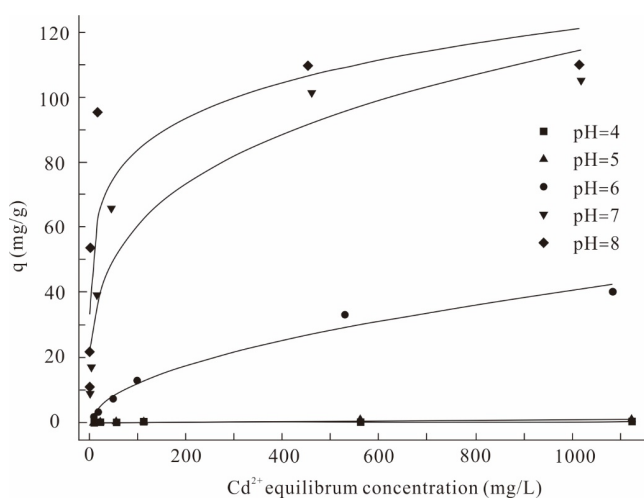


Fig. 6. Freundlich isotherm model fits to the cadmium sorption data (adsorbent dosage = 1 g/L, ionic strength = 0.01 mol/L, $T = 25^\circ\text{C}$, initial Cd^{2+} concentrations = 0.1–10 mmol/L, pH = 4.0–8.0).

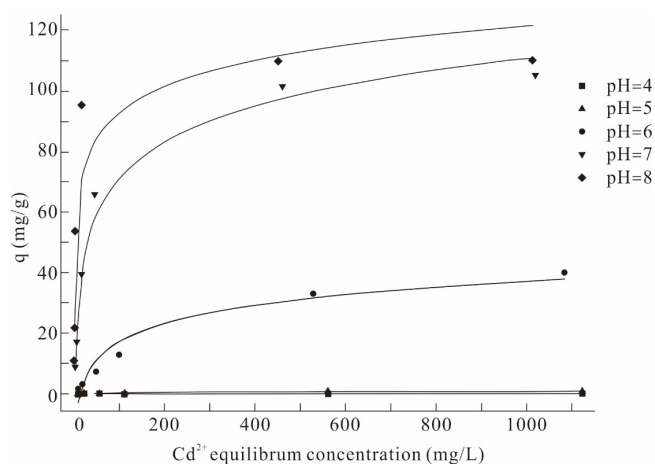


Fig. 7. Temkin isotherm model fits to the cadmium sorption data (adsorbent dosage = 1 g/L, ionic strength = 0.01 mol/L, $T = 25^\circ\text{C}$, initial Cd^{2+} concentrations = 0.1–10 mmol/L, pH = 4.0–8.0).

Table 1

Isotherm parameters at different pH. (adsorbent dosage = 1 g/L, ionic strength = 0.01 mol/L, T = 25°C, initial Cd²⁺ concentrations = 0.1–10 mmol/L, pH = 4.0–8.0)

pH	Langmuir			Freundlich			Temkin		
	q_{\max}	k	R^2	k	n	R^2	a	b	R^2
4.0	0.046	0.0003	0.97	0.0000	1.317	1.00	-0.0062	0.0021	0.84
5.0	1.028	0.0030	1.00	0.0194	1.868	0.96	-0.4858	0.1755	0.95
6.0	50.98	0.0034	1.00	1.0932	1.911	0.98	-22.3734	8.6078	0.95
7.0	107.86	0.0336	1.00	17.3803	3.675	0.91	-7.8538	17.1542	0.98
8.0	110.28	0.3756	1.00	40.4126	6.308	0.80	35.5816	12.4163	0.90

Table 2

A comparison of the Cd²⁺ adsorption capacities of various published adsorbents

Adsorbents	q_{\max} (mg/g)	References
Manganoxide	98	[31]
Activated carbon	47.85	[32]
Phosphogypsum	131.58	[33]
Perlite	0.64	[34]
Goethite	7.54	[35]
Clinoptilolite	7.41	[36]
Modified corncobs	9.0	[37]
Modified Pine bark	50.0	[38]
Macrofungus biomass	27.3	[39]
Granular red mud	6.69	[40]
Activated red mud	12.55	[41]
Polyphosphate-modified kaolinite clay	13.23	[42]
Manganese nodule residue	19.8	[43]
Fired coal fly ash	18.98	[44]
Coal combustion fly ash	4.3	[45]
Schwertmannite	110	–

and the adsorbate species speciation, which is a vital parameter in adsorption process [46,47]. Effect of initial solution pH on Cd²⁺ adsorption was carried out by using Cd²⁺ solutions with various initial pH between 4.0 and 8.0. As represented in Fig. 8, cadmium adsorption ratio steadily increased with the increase of pH, and decreased with the increasing Cd²⁺ concentrations, exhibiting typical pH edge curves. At an initial Cd²⁺ concentration of 0.1 mmol/L, cadmium adsorption ratio kept a relatively constant value at pH = 4.0–5.0, the cadmium adsorption rate was slightly increased at pH = 5.0–6.0, while at pH > 6.0 cadmium adsorption was dramatically increased. At pH = 8.0, nearly 100% cadmium was adsorbed. This phenomenon could be explained by the Cd²⁺ removal was suppressed by H⁺ at low pH. H⁺ surrounded the surface of the adsorbent, competed Cd²⁺ for the adsorption sites, hindering the approach of Cd²⁺ to the adsorption sites

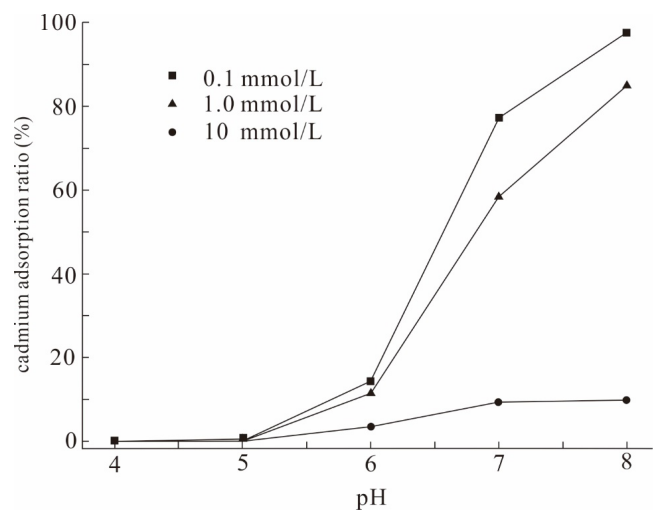


Fig. 8. Effect of pH on the adsorption of cadmium ion (initial Cd²⁺ concentration = 0.1–10 mmol/L, adsorbent dosage = 1.0 g/L).

[46]. When pH increased, the availability of H⁺ decreased leading to higher adsorption of Cd²⁺. This trend was similar to behavior of other adsorbents (such as ferrihydrite, goethite, zeolite, vermiculite, pumice, edible mushrooms [46–49]) in different pH. The increase of cadmium adsorption at higher pH might also be attributed to hydrolysis of Cd²⁺ (formation of Cd(OH)⁺ and Cd₂(OH)³⁺ and precipitation (Cd(OH)₂ ≥ 8.0) in aqueous solution, multivalent ions were adsorbed more readily at solution particle interfaces than non-hydrolyzed metal ions [49,50].

3.4. Effect of solution temperature

The effect of temperature on Cd²⁺ adsorption is shown in Fig. 9. Langmuir model was employed to describe the experimental data, giving higher correlation coefficients ($R^2 > 0.95$). Maximum removal capacities and K were 107.9 mg/g, 33.59 L/g at 25°C, and at 50°C, respectively, Maximum removal capacities and K are 108.9 mg/g, 56.41 L/g, indicating the increasing reaction temperature promote Cd²⁺ adsorption, which was an endothermic reaction.

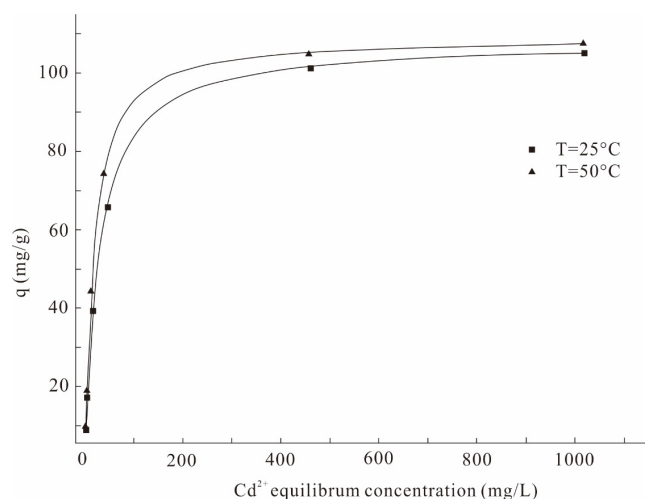


Fig. 9. Effect of temperature on the adsorption of Cd^{2+} (initial Cd^{2+} concentration = 0.1–10 mmol/L, adsorbent dosage = 1.0 g/L, ionic strength = 0.01 mol/L, pH = 7.0).

Table 3
Thermodynamic parameters of Cd^{2+} adsorption on synthetic schwertmannite

T (K)	ΔG (kJ/mol)	ΔH (kJ/mol)	ΔS (J/mol K)
298	-8.707	16.595	84.906
323	-10.829	16.595	84.906

To provide further insight into the mechanisms of Cd^{2+} adsorption, the thermodynamic parameters, including ΔG , ΔH and ΔS , were calculated, and the results were listed in Table 3. It was necessary to evaluate the thermodynamic feasibility and to confirm the nature of the adsorption process based on the determination of thermodynamic parameters. The Gibbs free energy change (ΔG in kJ/mol), is an indication of spontaneity of a reaction. It can be given by the following equation:

$$\Delta G = -RT \ln k \quad (5)$$

$$\Delta H = R \times \left(\frac{T_2 T_1}{T_2 - T_1} \right) \times \ln \frac{k_{T_2}}{k_{T_1}} \quad (6)$$

$$\Delta S = \frac{\Delta H - \Delta G}{T} \quad (7)$$

where R is the universal gas constant (8.314 J/mol K); T is absolute temperature (K); K is the adsorption equilibrium constant. The ΔG values were negative, and their absolute values increased with the increasing temperature, indicating that the adsorption process was spontaneous. The ΔS values were positive implied that the increase of temperature resulted in an increase in randomness of the systems, which was good for the Cd^{2+} adsorption. The positive ΔH

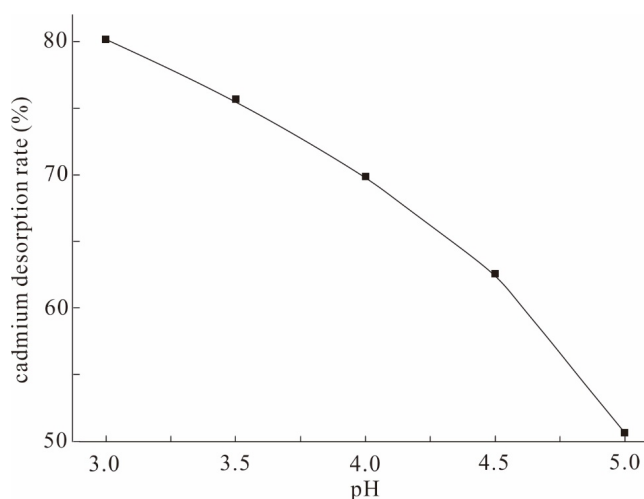


Fig. 10. Desorption of Cd^{2+} from schwertmannite as a function of pH (ionic strength = 0.01 mol/L, $T = 25^\circ\text{C}$, pH = 3.0–5.0).

values indicated an endothermic process, confirming Cd^{2+} adsorption isotherm experiments results that the values of q_{max} increased with the raising temperature.

3.5. The adsorption-desorption reaction

To test schwertmannite desorption ability of Cd^{2+} and regeneration ability, the experiment simulated the natural pH range for schwertmannite, and investigated the relationship between cadmium desorption rate and pH. The Fig. 10 showed that pH highly affected the desorption behavior of cadmium. Cadmium desorption rate decreased with increasing pH from 3.0 to 5.0. The desorption rate was 80% at pH 3.0, respectively 50.6% at pH 5.0. The solution with lower pH exhibited higher desorption ratio.

This indicated that the cadmium adsorbed schwertmannite had good regeneration ability in the natural environment acidity range for schwertmannite, and with pH decreased the desorption of cadmium improved. Schwertmannite had a good Cd^{2+} adsorption ability in pH 6.0–8.0, and it had strong regeneration ability with the reduced acidity. Therefore, schwertmannite can serve as an effective adsorbent to remove Cd^{2+} in water.

The phenomenon that cadmium desorbed rate decreased with increasing pH might be attributed to at low pH, high concentration of H^+ had competed successfully and rapidly with Cd^{2+} for adsorption sites on schwertmannite, releasing the Cd^{2+} [51, 52]. In addition, the instability of schwertmannite might have contributed to the desorption of Cd^{2+} . In low pH, the dissolution of schwertmannite could release the adsorbed Cd^{2+} , thus increased the cadmium desorption rate.

4. Conclusions

The texture and composition of synthetic schwertmannite were the same in the two methods (slow synthesis and rapid synthesis). But there existed a big difference in

schwermannite surface morphology. The rapid synthesis schwermannite grain size was large, and had a low crystallinity, respectively, the slow synthesis schwermannite was better crystallized and had a larger surface area than rapid synthesis. The batch results showed that the adsorption of Cd^{2+} fitted the Langmuir isotherm, which indicated that the monolayer adsorption mechanism. Thermodynamic study manifested that Cd^{2+} adsorption on synthetic schwermannite was spontaneous and endothermic. The synthetic schwermannite had high adsorption capacity for Cd^{2+} removal, which was up to 110 mg/g in the batch with an adsorbent dosage of 1 g/L and an initial pH 8.0 at 25°C. At pH > 6.0, cadmium adsorption was dramatically increased, nearly 100% cadmium was adsorbed at pH = 8.0. The Cd(II) adsorption on shoe waste adsorbent was investigated and conditions were optimized using RSM techniques under CCD statistical design in natural pH range for schwermannite, Cd^{2+} adsorbed schwermannite had a good regeneration ability, Cd^{2+} desorption rate was 50–80%, and the Cd^{2+} desorption rate increased with a decrease of pH. Therefore, schwermannite can serve as a good adsorbent of Cd^{2+} , and release adsorbed Cd^{2+} in low pH. The cadmium and schwermannite can be efficiently recycled due to the desorption ability of Cd^{2+} , which is environment-friendly.

Acknowledgments

Authors thank for Dr. Sun and Wu S for their helpful discussions and for providing kind assistance in experiments.

References

- J.L. Hu, X.W. He, C.R. Wang, Cadmium adsorption characteristic of alkali modified sewage sludge, *Biores. Technol.*, 121 (2012) 25–30.
- M.P. Waalkes, Cadmium carcinogenesis in review, *J. Inorg. Biochem.*, 79 (2000) 241–244.
- S.H. Yao, Z.R. Liu, Z.L. Shi, Adsorption behavior of cadmium ion onto synthetic ferrihydrite effects of pH and natural seawater ligands, *J. Iran. Chem. Soc.*, 11 (2014) 1545–1551.
- P. Das, S. Samantaray, G.R. Rout, Studies on cadmium toxicity in plants A review, *Environ. Pollut.*, 98 (1997) 29–36.
- S. Granero, J.L. Domingo, levels of metals in soils of alcalá de henares, Spain human health risks, *Environ. Int.*, 28 (2002) 159–64.
- Y. Fang, X. Sun, W. Yang, Concentrations and health risks of lead, cadmium, arsenic, and mercury in rice and edible mushrooms in China, *Food Chem.*, 147 (2014) 147–151.
- P. Grimshaw, J.M. Calo, G. Hradil, Cyclic electrowinning/precipitation (CEP) system for the removal of heavy metal mixtures from aqueous solutions, *Chem. Eng. J.*, 175 (2011) 103–109.
- C.W. Wong, J.P. Barford, G.H. Chen, G.M. McKay, Kinetics and equilibrium studies for the removal of cadmium ions by ion exchange resin, *J. Environ. Chem. Eng.*, 2 (2014) 698–707.
- S. Vasudevan, J. Lakshmi, Effects of alternating and direct current in electrocoagulation process on the removal of cadmium from water – A novel approach, *Separ. Purif. Technol.*, 80 (2011) 643–661.
- J. Kheriji, D. Tabassi, B. Hamrouni, Removal of Cd(II) ions from aqueous solution and industrial effluent using reverse osmosis and nanofiltration membranes, *Water Sci. Technol.*, 72 (2015) 1206–1216.
- K.J. Wang, B.S. Xing, Adsorption and desorption of cadmium by goethite pretreated with phosphate, *Chemosphere*, 48 (2002) 665–670.
- H. Nadaroglu, N. Celebi, E. Kalkan, The evaluation of affection of *Methylobacterium extorquens* – modified silica fume for adsorption cadmium (II) ions from aqueous solutions affection, *Kafkas Univ Vet Fak Derg*, 19 (2013) 391–397.
- M. Arias, M.T. Barral, J.C. Mejuto, Enhancement of copper and cadmium adsorption on kaolin by the presence of humic acids, *Chemosphere*, 48 (2002) 1081–1088.
- R. Kumar, J. Chawla, Removal of cadmium ion from water/wastewater by nano-metal oxides: a review, *Water Qual. Exposure Health*, 5 (2014) 215–226.
- T. Vidhyadevi, A. Murugesan, S.S. Kalaivani, Optimization of the process parameters for the removal of reactive yellow dye by the low cost *Setaria verticillata* carbon using response surface methodology thermodynamic, kinetic, and equilibrium studies, *Environ. Progr. Sustain. Energy*, 33 (2014) 855–865.
- S. Karthikeyan, M.A. Kumar, P. Maharaja, Process optimization for the treatment of pharmaceutical wastewater catalyzed by poly sulphate sponge, *J. Taiwan Inst. Chem. Eng.*, 45 (2014) 1739–1747.
- X.M. Dou, D. Mohan, U. Charles, J. Pittman, Arsenate adsorption on three types of granular schwermannite, *Water Res.*, 47 (2013) 2938–2948.
- S. Paikaray, J. Göttlicher, S. Peiffer, Removal of As(III) from acidic waters using schwermannite Surface speciation and effect of synthesis pathway, *Chem. Geology*, 283 (2011) 134–142.
- J. Jönsson, J. Sjöberg, L. Lövgren, Adsorption of Cu(II) to schwermannite and goethite in presence of dissolved organic matter, *Water Res.*, 40 (2006) 969–974.
- J. Antelo, S. Fiol, D. Gondar, Cu(II) incorporation to schwermannite effect on stability and reactivity under AMD conditions, *Geochim. Cosmochim. Acta*, 119 (2013) 149–163.
- A. Eskandarpour, M.S. Onyango, A. Ochieng, S. Asai, Removal of fluoride ions from aqueous solution at low pH using schwermannite, *J. Hazard. Mater.*, 152 (2008) 571–579.
- A. Goswami, M.K. Purkait, Removal of fluoride from drinking water using nanomagnetite aggregated schwermannite, *J. Water Process Eng.*, 1 (2014) 191–100.
- P. Zhou, Y.X. Shen, Y.Q. Lan, L.X. Zhou, Facilitating role of biogenic schwermannite in the reduction of Cr(VI) by sulfide and its mechanism, *J. Hazard. Mater.*, 237 (2012) 194–198.
- M. Gan, S. Sun, Z. Zheng, Adsorption of Cr(VI) and Cu(II) by AlPO_4 modified biosynthetic Schwermannite, *Appl. Surf. Sci.*, 356 (2015) 986–997.
- J.M. Bigham, U. Schwertmann, L. Carlson, E. Murad, A poorly crystallized oxyhydroxysulfate of iron formed by bacterial oxidation of Fe(II) in acid mine water, *Geochim. Cosmochim. Acta*, 54 (1990) 2743–2758.
- J.M. Bigham, L. Carlson, E. Murad, Schwermannite a new iron oxyhydroxysulfate from Pyhasalmi, Finland, and other localities, *Min. Mag.*, 58 (1994) 641–648.
- J.M. Bigham, U. Schwertmann, S.J. Traina, R.L. Winland, M. Wolf, Schwermannite and the chemical modeling of iron in acid sulfate water, *Geochim. Cosmochim. Acta*, 60 (1996) 2111–2121.
- J.M. Bigham, U. Schwertmann, L. Carlson, E. Murad, A poorly crystallized oxyhydroxysulfate of iron formed by bacterial oxidation of Fe(II) in acid mine waters, *Geochim. Cosmochim. Acta*, 54 (1990) 2743–2758.
- S. Regenspurg, A. Brand, S. Peiffer, Formation and stability of schwermannite in acidic mining lakes, *Geochim. Cosmochim. Acta*, 68 (2004) 1185–1197.
- Q. Liu, H.M. Guo, Y. Shan, Adsorption of fluoride on synthetic siderite from aqueous solution, *J. Fluor. Chem.*, 131 (2010) 635–641.
- A. Sönmezay, M.S. Öncel, N. Bektas, Adsorption of lead and cadmium ions from aqueous solutions using manganoxide minerals, *Trans. Nonfer. Metals Soc. China*, 22 (2012) 3131–3139.
- Z.F. Wang, E. Nie, J.H. Li, Y.J. Zhao, X.Z. Luo, Z. Zheng, Carbons prepared from *spartina alterniflora* and its anaerobically digested residue by H_3PO_4 activation characterization and adsorption of cadmium from aqueous solutions, *J. Hazard. Mater.*, 188 (2011) 29–36.

- [33] N. Balkaya, H. Cesur, Adsorption of cadmium from aqueous solution by phosphogypsum, *Chem. Eng. J.*, 140 (2008) 247–254.
- [34] T. Mathialagan, T. Viraraghavan, Adsorption of cadmium from aqueous solutions by perlite, *Chem. Eng. J.*, 94 (2002) 291–303.
- [35] I.K. Munther, Zinc and cadmium adsorption on low-grade phosphate, *Separ. Purif. Technol.*, 35 (2004) 61–70.
- [36] V.O. Vasylechko, G.V. Gryshchouk, Y.B. Kuz'ma, V.P. Zakordonskiy, L.O. Vasylechko, L.O. Lebedynets, M.B. Kalytovs'ka, Adsorption of cadmium on acid-modified transcarpathian clinoptilolite, *Micropor. Mesopor. Mater.*, 60 (2003) 183–196.
- [37] T. Vaughan, C.W. Seo, W.E. Marshall, Removal of selected metal ions from aqueous solution using modified corncobs, *Biores. Technol.*, 78 (2001) 133–139.
- [38] M.E. Argun, S. Dursun, Cadmium removal using activated pine bark, *J. Int. Environ. Appl. Sci.*, 3 (2008) 37–42.
- [39] A. Sari, M. Tuzen, Kinetic and equilibrium studies of biosorption of Pb(II) and Cd(II) from aqueous solution by macrofungus (*amanita rubescens*) biomass, *J. Hazard. Mater.*, 164 (2009) 1004–1011.
- [40] C.L. Zhu, K.L. Zhao, Q.W. Yan, D.S. Xing, Removal of cadmium from aqueous solutions by adsorption on granular red mud (GRM), *Separ. Purif. Technol.*, 57 (2007) 161–169.
- [41] M.K. Sahu, S. Mandal, L.S. Yadav, Equilibrium and kinetic studies of Cd(II) ion adsorption from aqueous solution by activated red mud, *Desal. Wat. Treat.*, 13 (2015) 1–15.
- [42] M.W. Amer, F.I. Khalili, A.M. Awwad, Adsorption of lead, zinc and cadmium ions on polyphosphate-modified kaolinite clay, *J. Environ. Chem. Ecotoxicol.*, 2 (2010) 1–8.
- [43] A. Agrawal, K.K. Sahu, Kinetic and isotherm studies of cadmium adsorption on manganese nodule residue *J. Hazard. Mater.*, 137 (2006) 915–924.
- [44] A. Papandreou, C.J. Stournaras, D. Pantias, Copper and cadmium adsorption on pellets made from fired coal fly ash, *J. Hazard. Mater.*, 148 (2007) 538–47.
- [45] M. Balsamo, F.D. Natale, A. Erto, Cadmium adsorption by coal combustion ashes-based sorbents – Relationship between sorbent properties and adsorption capacity *J. Hazard. Mater.*, 187 (2011) 371–378.
- [46] M.R. Panuccio, A. Sorgonà, M. Rizzo, G. Cacco, Cadmium adsorption on vermiculite, zeolite and pumice: batch experimental studies, *J. Environ. Manage.*, 90 (2009) 364–374.
- [47] S. Yao, Z. Liu, Z. Shi, Adsorption behavior of cadmium ion onto synthetic ferrihydrite: effects of pH and natural seawater ligands, *J. Iran. Chem. Soc.*, 11 (2014) 1545–1551.
- [48] G. Mustafa, B. Singh, R.S. Kookana, Cadmium adsorption and desorption behaviour on goethite at low equilibrium concentrations: effects of pH and index cations, *Chemosphere*, 57 (2004) 1325–1333.
- [49] T. Mathialagan, T. Viraraghavan, D.R. Cullimore, Adsorption of cadmium from aqueous solutions by Edible Mushrooms (*agaricus bisporus* and *lentinus edodes*), *Water Qual. Res. J. Canada*, 38 (2003) 499–514.
- [50] J. Liang, J. Liu, X. Yuan, Facile synthesis of alumina-decorated multi-walled carbon nanotubes for simultaneous adsorption of cadmium ion and trichloroethylene, *Chem. Eng. J.*, 273 (2015) 101–110.
- [51] X. Yang, Z. Hu, A. Gao, Y. Zhu, Study on adsorption of Cd²⁺ with Na-modified bentonite, *Environ. Chem.*, 23 (2004) 506–509.
- [52] S. Wen, D. Yang, J. Chen, X-Ray diffraction characterization of bentonite, acidation bentonite and alkalization bentonite and surface characters under scanning electron microscope (SEM), *Acta Mineralog. Sinica*, 21 (2001) 453–456.